Enceladus Close Up:
New Details Recovered from Cassini ISS Boresight-Drag Images

Paul Helfenstein, Peter C. Thomas, Joseph Veverka

Center for Radiophysics and Space Research, Cornell University, Ithaca, NY 14853-6801

abstract

Among the many Cassini ISS (Imaging Science Subsystem) images of Enceladus are a few severely-underexposed, motion-blurred images that were acquired on "boresight-drag" events on the closest flybys. During boresight-drags, ISS is statically aimed at a point that intercepts the predicted path of Enceladus' across the sky. The ISS Narrow angle (NAC) and Wide Angle (WAC) cameras are repeatedly triggered together in hope of serendipitously capturing a close-up "BOTSIM" image-pair of the body as it passes. Because the events are so fast, the surface footprints and lighting geometry cannot be predicted in advance – a cascade of images are just quickly shuttered at the minimum 5 ms exposure. On each of four boresight-drags, surface images were captured. However, the two most recent (image-pair W/N1669812043 in November 2010 and W/N1713106405 in April 2012, respectively) were poorly illuminated -- three of four images only in Saturnshine. Despite their poor signal quality, they are rare images of Enceladus' surface obtained with spatial resolutions better than a few meters/pixel. Careful use of Fourier filtering and spatial reconstruction techniques was needed to eliminate image noise and residual electronic banding that was not removed during routine radiometric calibration of the images. Fourier motion deblurring techniques were then applied to correct for significant motion smear.

Images W/N1669812043 (55.1°N, 20.2°W) are in old cratered terrain, inside a prominent 23 km sized impact crater along the rise of its updomed floor. They show a system of parallel ~250m wide mesas trending around the dome's circumference. Smooth detritus inundates mesas and valleys near the dome summit and the mesa surfaces are otherwise mantled with regolith that is finely cratered down to the ~2 m/pixel NAC resolution limit. W/N1713106405 (66.9°S, 29.5°W) show the chaotically fractured margin of the active South Polar Terrain – an area divided by parallel ridges and troughs with relatively smooth flanks and valley floors. Quasi-linear arrangements of ice-blocks, each block tens of meters or smaller, are found mostly near ridge-tops.

Spatial Filtering and Noise Reduction

When an image is obtained under conditions for which the spacecraft cannot accurately track the target, motion blur can significantly degrade the image quality and may severely reduce feature definition. In addition, in a severely underexposed, low-signal image, electronic noise, such as coherent horizontal banding and vertical banding and random noise from radiation and other causes can obscure real features in the imaged scene. To recover details in our highest-resolution images, we apply two-dimensional Fast Fourier Transform (FFT) signal filtering, which has long been the most successful, widely-used approach for removing periodic an other noise from digital images (cf. Jensen 1968). We divide the approach into correction for blurring due to camera motion, spatial filtering to remove periodic electronic noise, filtering of random noise and other non-systematic artifacts, and merging of high-resolution details from Cassini Narrow Angle Camera (NAC) with low-resolution scene elements from the Wide Angle Camera (WAC) when BOTSIM images are available.

Motion Blur Correction: In principle, blurring of an image due to uniform motion should be relatively easy to treat with Fourier methods given knowledge of the magnitude and direction of the smearing motion. The transfer function in this case should be the Fourier transform of a star-image (or single point) that has been artificially smeared by the known length in pixels in the direction of camera motion. A more complicated transfer function would be needed if the camera motion was non-uniform. Random noise and sharp brightness boundaries in an otherwise bland scene can also introduce serious artifacts. Consequently, sophisticated refinements of Fourier motion deblurring have been developed (cf. Shan et al. 2008; Xu and Jiaya, 2010).

We have tested a variety of these methods on a case-by-case basis and we chose the best result when a sophisticated approach yielded significant improvement over the simple method. Fig. 1 shows a section of WAC image W1713106405 (from observation sequence ISS_164EN_ENCEL18001_INMS) which had four pixels of motion blur (left-panel) and after deblurring (right-panel). The spacecraft motion produced 1.5 pixels in the horizontal image direction and 4.5 pixels in the vertical image direction. The sunlit parts of this image are illuminated well-enough for good signal-to-noise characteristics and extra processing to remove periodic noise wasn't necessary. Features as small as 10 meter sized ice-blocks are visible in both panels, but the features are crisper in appearance and more defined in the desmeared image. Desmearing has also revealed a set of parallel, diagonally cross-cutting lineaments on the bright valley wall near the bottom of the picture.

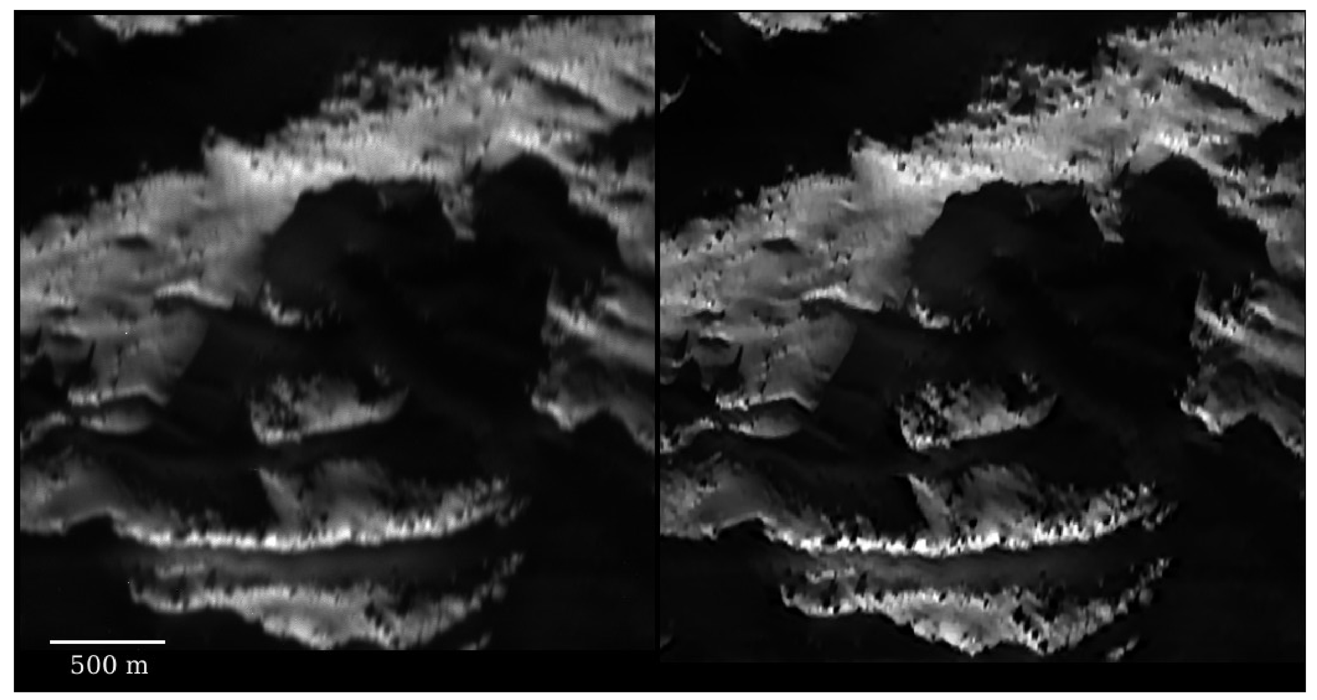

Figure 1: Correction of motion blur in WAC CL1-CL2 filter image W1713106405. *Left*) A 512x512 pixel section of the spatially uncorrected (i.e. blurred) image that was obtained during a drag of the WAC boresight over the south polar region of Enceladus. The image has been radiometrically calibrated with CISSCAL, but it is otherwise uncorrected. Image is smeared horizontally by 1.5 pixels and vertically by 4.5 pixels. *Right*) Left image after correcting for motion blur. Because no pre-filtering of noise was done prior to deblurring, an iterative approach was used to minimize noise artifacts (Xu and Jiaya 2010).

Periodic Noise Removal: The most prominent periodic electronic noise in ISS NAC and WAC images is a 2 Hz coherent noise pattern (Porco *et al.* 2004) that appears as horizontal banding in the images (see *Fig. 2a*). Routine radiometric calibration of the images by the CISSCAL computer program (Knowles 2012) removes a significant component of this noise, leaving only very low-amplitude residual banding artifacts (*Fig. 2b*). However, as seen in Fig. 2b, residual horizontal banding is still significant in the CISSCAL processed BOTSIM WAC image from the E12 close-flyby ISS_141EN_GRAVITY002_RSS. Fig. *2c* shows the unfiltered Fourier transform amplitude image. In this representation, the lowest spatial frequency (the average image brightness or "DC-term") is at the center of the FFT image, and spatial frequencies increase with distance from the center. A vertical notch-filter (Fig. *2d*) is used to mask spatial frequencies that generate the horizontal banding. While the original banding in the raw WAC image (Fig. *2a*) is relatively uniform and its discrete component spatial frequencies and overtones might be predictable from theory, the residual artifacts in the calibrated images are much less uniform so that a relatively narrow notch in an otherwise solid bar is needed to filter out the wide range of band frequency components. Fig. *2e* shows the spatial noise in image space that is removed by application of the notch filter and Fig. *2f* shows the calibrated image after subtracting the periodic noise. The filtered image is grainy because the short camera exposure provided only a few levels of DN quantization over the scene, and these were not strongly elevated above the DN level of random background noise. Fig. 3 shows more sophisticated periodic noise removal in the NAC image.

Removal of Random Noise and other Non-Periodic Noise: Additional, more sophisticated spatial noise filtering significantly improves the end result of periodic noise removal (Fig. 4). To remove random noise, a low-pass filter (known as a Butterworth filter) is used (bright spherical shape in the center of *Fig. 4b*). To remove the grass-like noise patter, we superpose an hour-glass shaped low-pass filter within the Butterworth-filter and apply it to the FFT. The optimal diameter of the filter in Fourier space is found by trial-and-error. The noise removed by this composite spatial filter is shown in *Fig. 4c*, and the filtered image itself is shown in *Fig. 4d*.

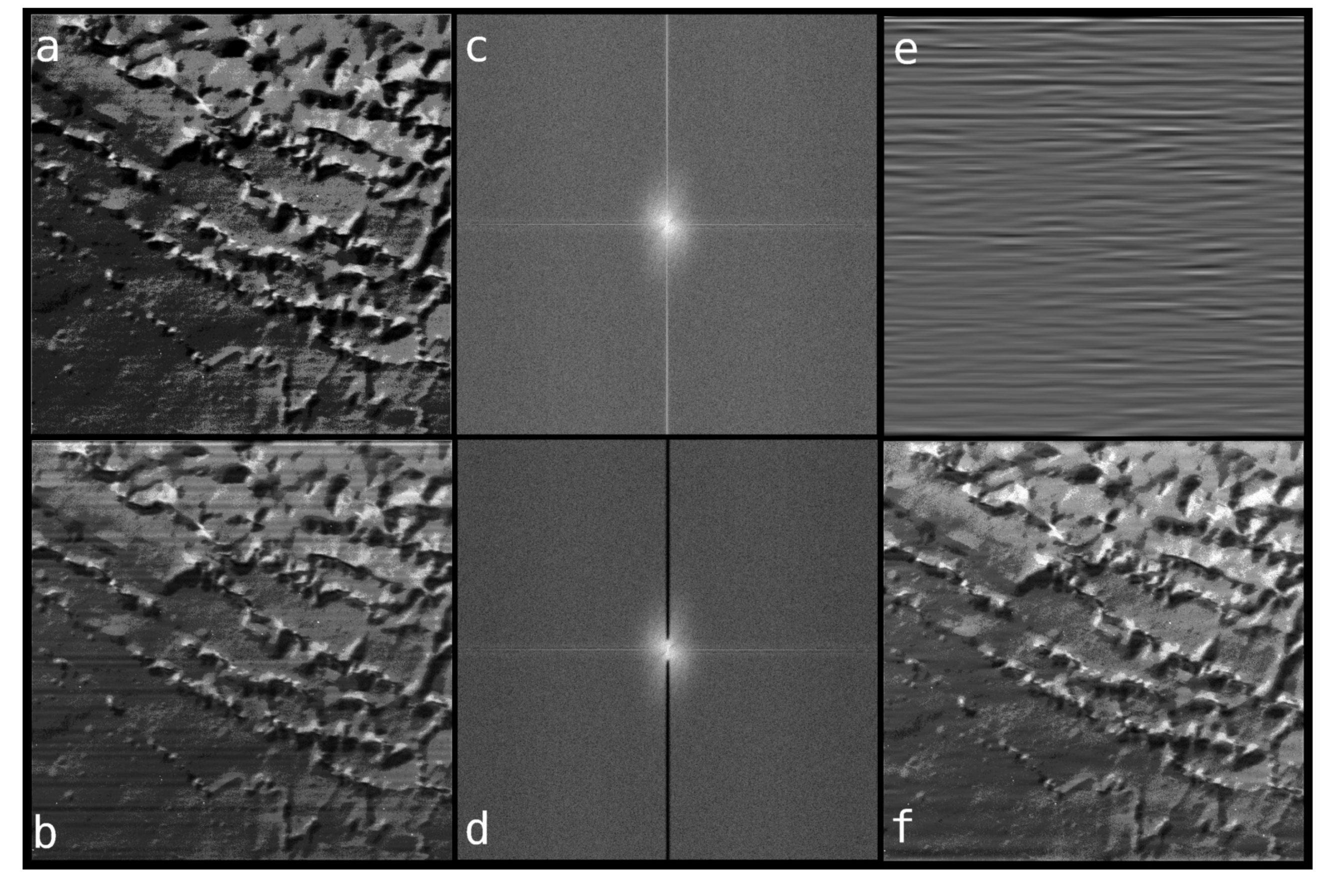

Figure 2: Periodic noise removal from WAC image W1669812043. a) Raw, unprocessed image except for contrast stretching to reveal image content. Periodic noise is seen as relatively uniform horizontal banding superposed over the scene. The short (5 ms) exposure resulted in poor signal-to-noise characteristics, evident from the coarse quantization of DN levels and the poor spatial definition of geological features. b) Image after radiometric calibration with CISSCAL. The systematic noise has been reduced in intensity relative to the Enceladus scene brightness. However, residual banding artifacts are still present as narrow quasi-horizontal bands. c) Fast Fourier Transform (FFT) of the calibrated image. Only the amplitude (real) component of the FFT is shown. Nearly all of the residual periodic noise in the calibrated image is horizontal banding that can be filtered in frequency space by masking information content along the vertical vane of the bright central star-shaped axial spectrum. d) Application of a notch-filter (dark vertical bar that is split in the center) to the FFT of calibrated image. (Note: FFT amplitude images in *c* and *d* have been separately contrast-enhanced for presentation in the figure). e) Image showing the noise that is removed by the notch-filter. f) Image after filtering and periodic noise removal with the notch-filter. Random noise and graininess is still present in the filtered image; it can be reduced with careful application of a low-pass spatial filter.

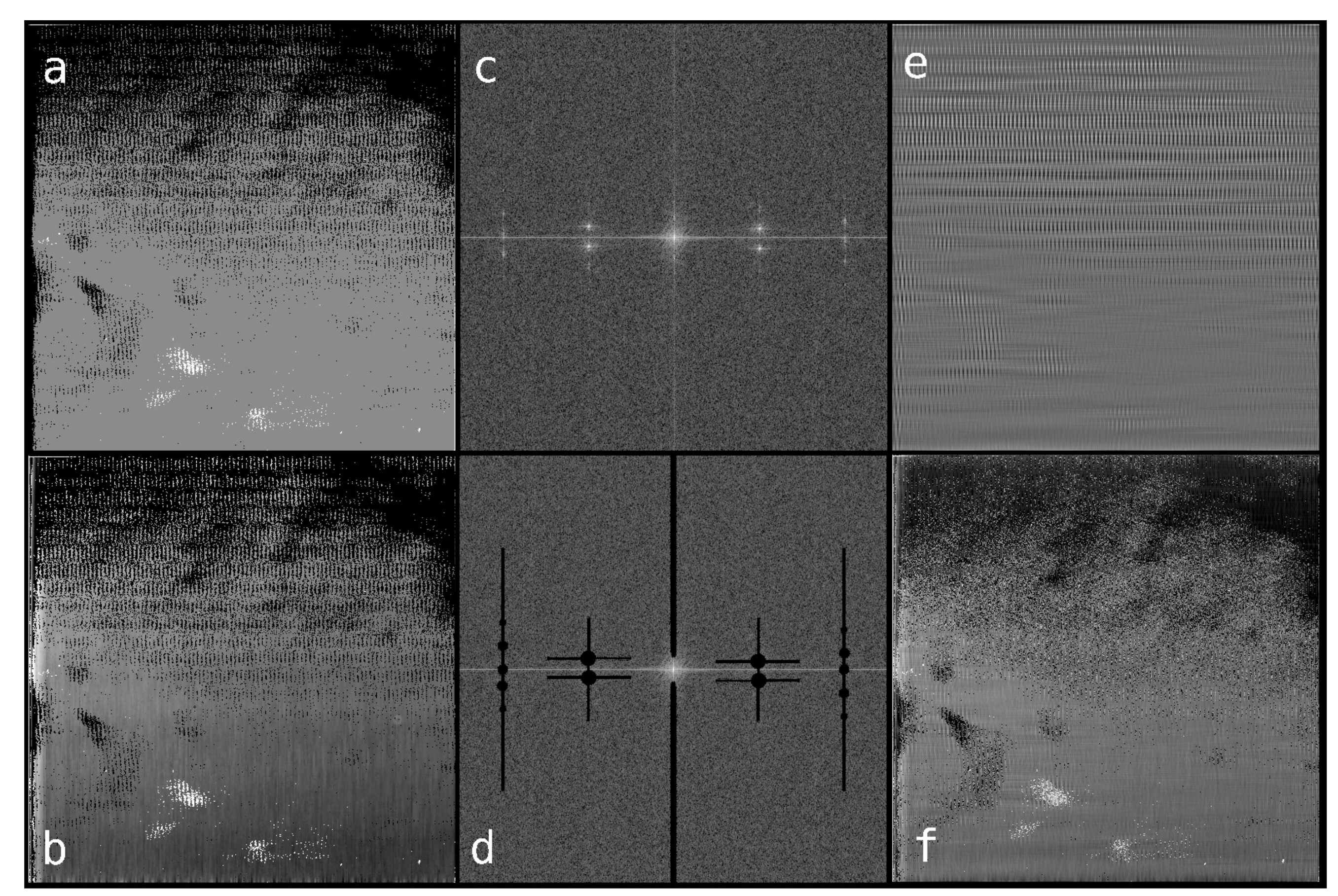

Figure 3: Periodic noise removal from NAC image N1669812043. a) Stretched, raw image. The signal-to-noise characteristics of this image are very poor and the pattern of periodic noise is complicated, hash-like with both broad horizontal and closely-space vertical banding superposed over the scene. b) CISSCAL and slightly reduced the systematic. c) FFT of the calibrated image. A conspicuous, almost symmetric series of star-like features flank and cross-cut the horizontal axis of the transform spectrum and fairly regular intervals -- FFT expressions of simultaneous vertical and horizontal. d) Application of a composite spatial filter to the FFT in c. A range of "star-filters" , "post-filters', and "notch filters" have been applied to mask-out the spatial spectral components of orthogonal banding. e) Spatial domain image showing the noise component that is removed by the filter arrangement in *d*. f) Spatial domain image created by inverse transform of the applied spatial filter arrangement in *d*. Intense graininess from random noise is still present in the filtered image and the lower-half of the image remains obscured by the non-uniform grassy pattern of noise. However, the visibility of craters and topographic structures has been significantly improved.

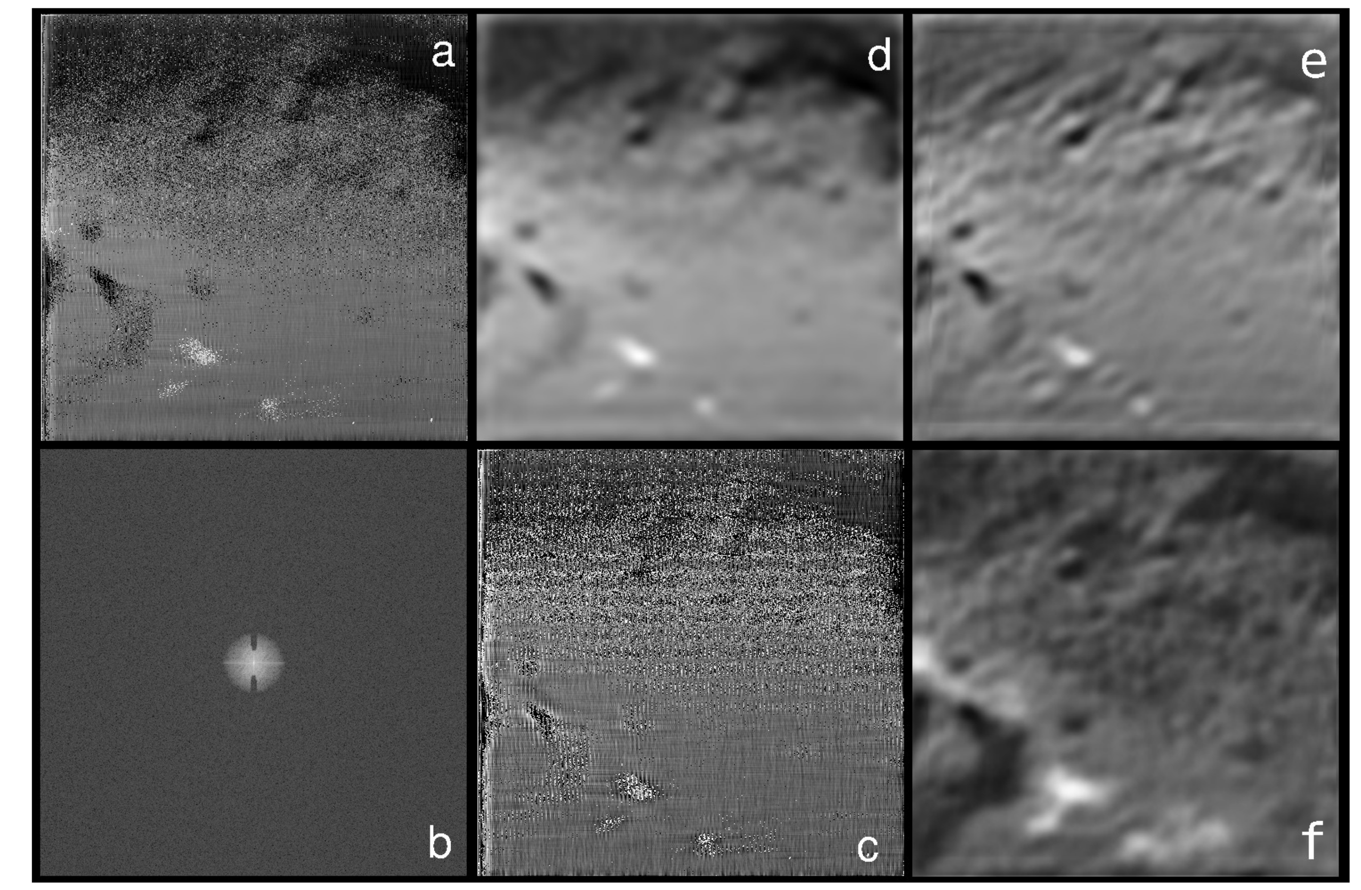

Figure 4: Spatial filtering of random noise in NAC BOTSIM image N1669812043. a) Same as Fig. 3 -- a calibrated image that that has already been spatially filtered to remove periodic noise. b) Modified Butterworth low-pass filter (see text) applied to the FFT of image in *a.* A small section of the frequency spectrum shows data that have already been masked-out by the notch-filter in *Fig. 3d*. c) Spatial domain image that shows the noise that is removed by the applied low-pass filter arrangement *b*. A few crude crater-patterns in the upper half of the noise-image indicate that a minor amount of real spatial detail has been filtered-out with the noise. d) Image after application of the low-pass filter, e) image after desmearing, f) desmeared image registered and merged with corresponding section of WAC image W1669812043. The image mainly shows surface-relief, with virtually no albedo information. Numerous small impact craters are evident, especially in the top half of the frame. Due to the poor signal strength in the original image and some motion blur, the predicted spatial resolution limit of 720 cm/pixel was probably not realized. However, where details are present, they likely present spatial resolution that is a factor of two or better than the resolution of the BOTSIM WAC image alone.

Results in Context

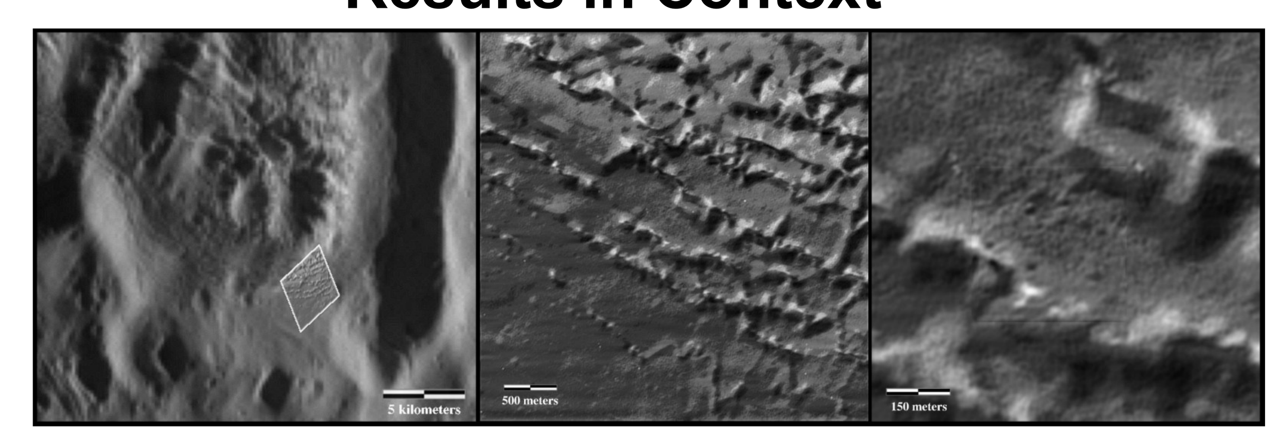

Figure 5: BOTSIM observation ISS_141EN_GRAVITY002_RSS. Left) Footprint of WAC image at (55.1°N, 20.2°W) relative to updomed crater floor. Images W/N1669812043 are in old cratered terrain, inside a prominent 23 km sized impact crater along the rise of its updomed floor. They show a system of parallel ~250m wide mesas trending around the dome's circumference. Smooth detritus inundates mesas and valleys near the dome summit and the mesa surfaces are otherwise mantled with regolith that is finely cratered down to the ~2 m/pixel NAC resolution limit. Center) WAC image resolution is ~6 m/pixel., Right) NAC image resolution is slightly poorer than theoretical 0.6 m pixel .

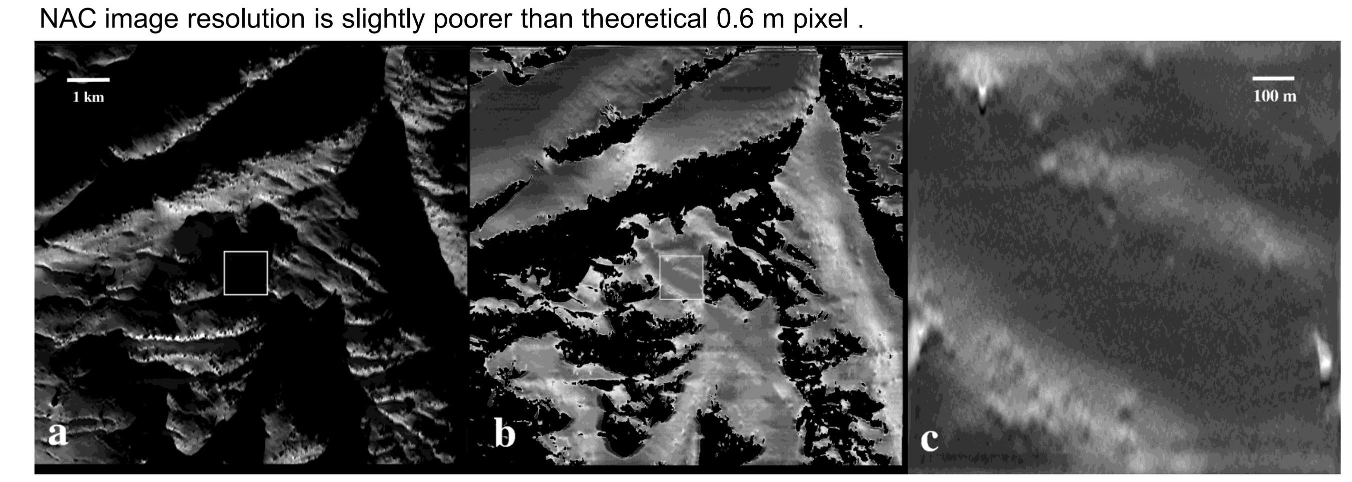

Figure 6: BOTSIM observation ISS_164EN_ENCEL18001_INMS at (66.9°S, 29.5°W). a) W/N1713106405 show the chaotically fractured margin of the active South Polar Terrain – an area divided by parallel ridges and troughs with relatively smooth flanks and valley floors. Quasi-linear arrangements of ice-blocks, each block tens of meters or smaller, are found mostly near ridge-tops. b) Same as a but contrast stretched to show shadowed area (6 m/pixel), c) NAC image (0.6 m/pixel).

This research was supported by NASA's Cassini Mission, ISS Team.